Proceedings of the 9th International Conference on Physical Modelling in Coastal Engineering (Coastlab24)

Delft, Netherlands, May 13-16, 2024

Conference Paper, DOI: 10.59490/coastlab.2024.684

SMALL-SCALE EXPERIMENTAL EVIDENCE ON THE USE OF DATE PALM FOREST TO MITIGATE TSUNAMI IN THE ARABIAN SEA

N.A.K. NANDASENA

United Arab Emirates University, United Arab Emirates, n.nandasena@uaeu.ac.ae

ABSTRACT

Because of the multi-scale benefits, ecosystem-based disaster risk reduction (Eco-DRR) has received much attention in coastal disaster mitigation. Coastal forests are considered a sustainable and economical solution to mitigate inundations from tsunamis. Owing to the rare occurrence of tsunamis and reported local tsunami heights being small, the coastal forests are a potential solution to protect from tsunamis in the Arabian Sea. The potential of date palm trees to mitigate tsunami inundations was investigated in an experimental study. The experiments were conducted at a geometric scale of 1:100 with the Froude-Cauchy similitudes. It found that the canopy of the tree played a key role in flow energy reduction. If the tsunami height was higher than the canopy height a significant tsunami depth was reduced behind the forest compared to the case that the tsunami height was lower than the canopy height. The highest percentage reduction in the maximum flow depth behind the forest was 37% for the forest length of 180 m and tsunami height of 7 m.

KEYWORDS: Date palm, tsunami, mitigation, experiment, Middle East

1 INTRODUCTION

Coastal lands have experienced rapid development in recent decades. However, climate warming and sea level rise increase the chances of extreme marine flooding that can damage coastal areas frequently in the future (Rovere et al., 2017). The countries bordering the Arabian Sea are at tsunami risk from the Makran subduction zone (MSZ) (Jordan, 2008). Over the past centuries, several tsunamigenic events have been triggered by the MSZ, including earthquakes in 1756, 1851, and 1945. The 1945 Mw 8.1 earthquake is the largest instrumentally recorded earthquake in the area (Byrne et al., 1992) that generated tsunami waves in the Arabian Sea. The destructive tsunami in 1945 was responsible for the deaths of more than 4,000 people in Southern Pakistan but also caused a severe impact on the coasts of Western India, Iran, and Oman (Pararas-Carayannis, 2006). A viable method of determining the hazards posed by tsunamis is to numerically predict their propagation using data on undersea earthquakes and landslides (Sarker, 2017). According to Suppasri et al. (2016), tsunami waves of 0.3 to 3.5 m high can be produced along the coast of the United Arab Emirates by a subsurface earthquake with a magnitude of 8.3–9.0 Mw and related surface landslides with a volume range of 0.5–1.0 km^2. Similar research conducted in 2020 by Nouri et al. (2020) revealed that waves as high as 24 meters might be produced in Muscat, Oman, by an underwater landslide measuring 4.5 km long, 4 km wide, and 0.6 km thick. The maximum run-up and depth of flow on the Diba coast were 1.16 m and 1.37 m, respectively, from an 8.8 Mw earthquake that originated in the eastern Makran Subduction Zone. On the other hand, an 8.2 Mw earthquake that originated in the western Makran Subduction Zone caused a maximum run-up of 2.57 m and a depth of flow of 2.34 m (El-Hussain et al., 2017). As per Rashidi et al. (2022), the likelihood of tsunami waves in the Gulf of Oman surpassing 1 m and 3 m in 250 years is 1 and 0.8, respectively. The investigation of past tsunami occurrences in the Arabian Sea depends on paleo-sediment deposits (Hoffmann et al., 2015). Low-energy wave occurrences cannot move isolated rocks up to 40 tons in weight in Fins and Sur, Oman (Hoffmann et al., 2013). An ancient tsunami from the Makran Subduction Zone may have flooded Ras al-Hadd, Oman, according to a coexisting sand bank with a maximum thickness of 0.4 meters (Hoffmann et al., 2015). Koster et al. (2014) also documented marine deposits with coarse to fine grains in Fins, Oman, an area where normal seas and swelling wave occurrences prevent the creation of such formations. Griffis (2018) discovered seven overwash strata beneath the 1945 Makran tsunami deposits, indicating previous high-energy marine inundations in Sur and throughout Oman. The field data, numerical predictions, and high-energy wave deposits in the Arabian Sea inform the possibility of the occurrence of tsunamis in the Arabian Sea in the future.

Therefore, developing mitigation methodologies for tsunami mitigation in the Arabian Sea is essential. Ecosystem-based disaster risk reduction (Eco-DRR) is the sustainable management, conservation, and restoration of ecosystems to provide

services that reduce disaster risk by mitigating hazards and by increasing livelihood resilience (Estrella and Saalismaa, 2013). Coastal forests are some of the most diverse ecosystems in the world. Coastal forests (planted or naturally grown) protect coastlines from storms and erosion. A substantial amount of research in field survey, numerical, and experimental studies was carried out following the 2004 Indian Ocean tsunami to examine the effectiveness of coastal vegetation, including hybrid defenses for minimizing the impact of tsunamis to protect lives and infrastructure (Danielsen et al., 2005; Kathiresan and Rajendran, 2005; Harada and Imamura, 2005; Tanaka and Sasaki, 2007; Tanaka et al., 2006, 2007; Nandasena et al., 2008; Tanaka et al., 2011; Iimura and Tanaka, 2012; Samarakoon et al., 2013; Tanaka et al., 2014; Rodríguez et al., 2016; Tanaka and Onai, 2017; Tanaka et al., 2018; Torita et al., 2022). The research informed that the protection provided by coastal forests depends on the local tsunami magnitude at the forest, the characteristics of vegetation such as the extent of the forest, the density and the vertical configuration of a tree, root-soil interaction, the distance to the shore, and the ground slope. The Middle East has a hot, arid, and semi-arid desert climate. However, a limited number of tree species such as date palm trees are extensively grown in the desert climate and they are tolerant to salinity. The strong stem, the roughness of the tree surface, and the strong connection with soil are good indicators that date palm forests can dissipate the energy of tsunami flooding. However, no studies have been conducted to elucidate the effectiveness of date palm trees in mitigating tsunami flows. In this study, the capability of date palm trees to mitigate tsunami energy was tested in small-scale experimental studies.

2 METHODOLOGY

1.1 Properties of date palm trees

Growing for at least 5,000 years throughout North Africa and the Middle East, the date palm tree (Fig. 1) is considered to be one of the earliest fruit crops ever planted by humans (Chao and Krueger, 2007). Date palms may reach a height of 20 meters. The tree roots can extend more than 6 meters below the palm and up to 25 meters below it. Most of them are located in deep loamy soil in a zone that is 2 m deep and 2 m on both lateral sides (Munier, 1973). Date tree trunks are columnar, upright, cylindrical, and have uniform girth. They go by the names stems and stripes as well. Upon reaching full development of the frond canopy, the girth stops growing. It has no ramification, is brown, and is lignified. Its average circumference is between 1 and 1.1 meters. The average properties of date palms are tree height of 6 – 40 m, diameter of 0.3 – 0.6 m, and spacing of 7 – 10 m (Jahromi et al., 2007). While date palms' Young's modulus ranges from 10 to 30 GPa (Amroune et al., 2015; Chihaoui et al., 2020), their tensile strength varies from 58 to 203 MPa (Jonoobi et al., 2019). The date palms hold great potential for usage as a coastal bio-shield to reduce tsunamis due to their remarkable mechanical qualities, longevity, resistance to salinity, notable height, robust root system, and rough surface. Coconut, pine, casuarina, pandanus, and mangroves have been adopted to mitigate tsunamis in other climatic and geographic conditions in other parts of the world (Fig. 1). The date palm tree's stand structure is comparable to that of a coconut tree, while mangrove and pandanus trees are more densely populated than date palms. Coconut, pine, casuarina, and mangrove trees have average Young's moduli ranging from 3 to 15 GPa (Bather et al., 2008; Nurulaini et al., 2013; Zhang et al., 2015; Pestka et al., 2019) that are analogs to date palm trees.

Figure 1. Vertical configuration of date palm in comparison to other trees used for tsunami mitigation. Photos from Left to Right (date palm, coconut, casuarina, pine, pandanus, and mangrove).

1.2 Experimental setup

Experimental studies were conducted at the United Arab Emirates University. Geometric similarity and Froude-Cauchy similitude were considered to maintain the similarity of flow depth, flow velocity, vertical configuration, and rigidity of date palm trees between the prototype and model. The geometric scale of the experiment was 1:100. Selecting mature date palm trees, the characteristics of a model tree were set as tree height of 9 cm (stem height of 6 cm, crown height of 3 cm), crown width of 6 cm, spacing between two trees of 6 cm, and tree diameter of 6 mm. The trees were fixed for the staggered pattern to get the maximum density (Fig. 2). The trees were firmly glued to the base therefore the root-soil interaction and scour around the trees during tsunami inundation were not modelled in this study. The characteristics of tsunami flow and

mechanical properties of date palm trees confirmed that the Cauchy number was in the order of 10^7 for both the model and prototype. The experiments were conducted in a dam-break flume that was 3 m in length, 0.5 m in depth, and 0.4 in width (Fig. 3).

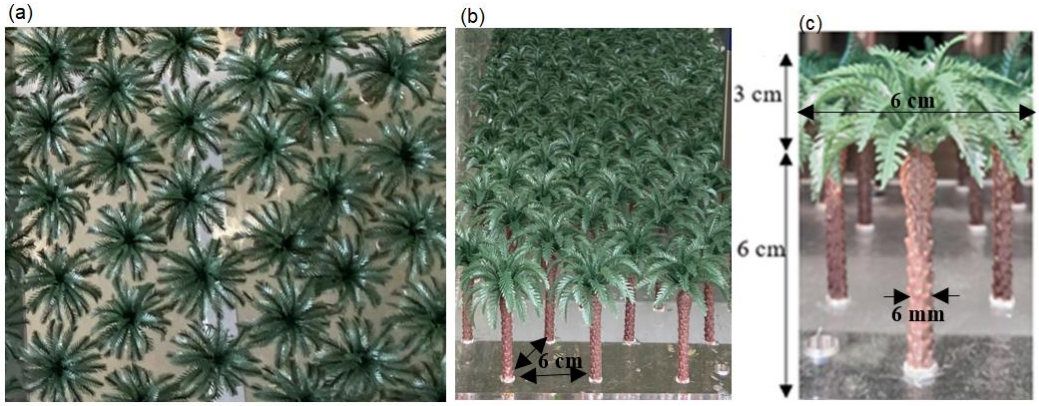

Figure 2. Date palm tree models (a) plan view of the model forest, (b) side view of the model forest, and (c) vertical configuration of a model tree.

Following past studies (Nandasena and Tanaka 2013; Xu et al. 2021), tsunami-like inundations over the forest model were generated by quickly releasing a water volume retained upstream of the flume. A special lever method was adopted to open the gate by giving a lesser torque on the arm (Fig. 3). It was assumed that the simulated inundation corresponded to the highest wave in the wave train and that it arrived first. Hence, a single flow was considered in each test. The downstream of the flume was kept open so that water drained out of the flume in each experiment. Therefore, the return flow was not considered.

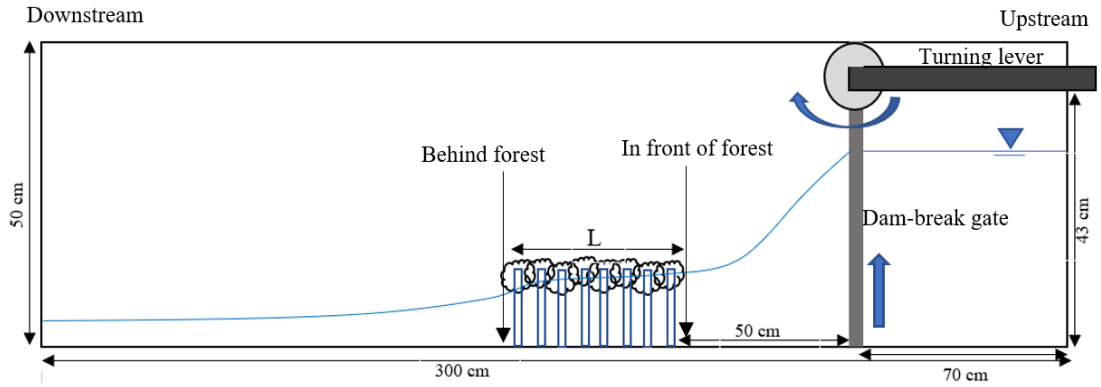

Figure 3. Experiment set-up. L is the forest length in the flow direction. The location of the forest front was fixed but the location of the forest end changed with the forest length (L).

Six tsunami heights up to 7 m were considered based on field data after the 1945 Makran tsunami, numerical modeling, and statistical analysis of past studies on tsunamis in the Arabian Sea. The maximum flow depth at 50 cm in front of the dam-break gate represented the tsunami height without the date palm forest (control) and it was generated by setting the required water level in the upstream tank (Fig. 3). Fig. 4 shows the relationship between the maximum flow depth and tank water depth. The maximum flow depth increased with the tank water depth. The calibration curve in Fig. 4 was used to generate the required maximum flow depths (2, 3, 4, 5, 6, and 7 cm) in the experiment. Six lengths of the forest (L in Fig. 3), ranging from 30 cm to 180 cm in 30 cm increments were considered parallel to the direction of flow. The depths and velocities of flow in front of and behind the forest were measured with and without the presence of the forest models. The maximum depth of flow was read by using a scale and the maximum velocity of flow was calculated from the time series recorded by an electromagnetic current meter at 20 Hz (JFE Advantech Co., Ltd. ACM2–RS; accuracy, ±0.5 cm/s). A total of 36 cases (six maximum flow depths and six lengths of the forest; for each maximum flow depth six lengths of the forest) were tested. Each test was repeated at least three times and the average measurements were considered for analysis. The maximum depth of flow in front of the forest was compared with that under the no-forest condition to investigate the effect of the forest in blocking/reflecting the flow as this controls the inundation distance of the tsunami. The maximum depth and velocity behind the forest were compared to the corresponding without-forest cases to elucidate the tsunami energy reduction by the forest. Moreover, video footage was used to explain the tsunami-forest interaction qualitatively.

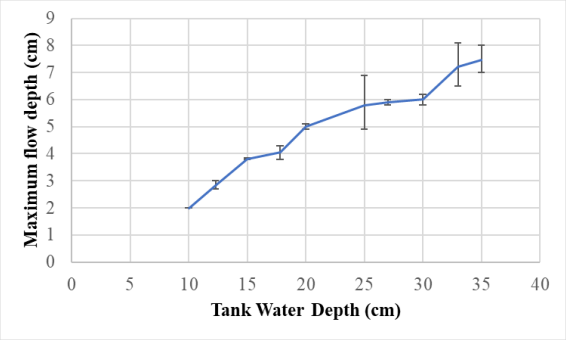

Figure 4. Flume calibration curve.

2 RESULTS

The results were explained in prototype values.

2.1 Flow characteristics over the forest

Fig. 5 shows the spatial variation in the depth of flow through the shortest forest (30 m) for the minimum and maximum tsunami waves (2 and 7 m in front of the forest). The depth of flow through the 30-m-long forest was nearly 2 m, the same as the height of the tsunami wave.

Figure 5. Tsunami inundation over the smallest forest (30 m in length). Left: tsunami height of 2 m; Right: tsunami height of 7 m.

This indicates that the stems of date palm trees were not effective at mitigating the height of the tsunami. However, when a 7-m-high tsunami waves hit the forest a gradient in the level of water was observed through the forest, therefore, a significant flow depth reduction behind the forest. When the flow interacted with the canopy of the tree, a turbulent-like flow structure was generated at the canopy but it was not significant through the stems of the trees. The forest was engulfed by the flow, and both the stems of trees and their canopy blocked the path of flow, which increased the water depth in the front of the forest than behind it. This indicates that the canopies of the date palm trees were more effective in blocking flow than their stems when the tsunami wave was higher than the canopy height. Therefore, even a short forest of date palm trees can reduce the energy of high tsunamis to some extent. Fig. 6 shows the spatial variation in the depth of flow through the longest forest (180 m) in the case of a 7-m-high tsunami wave.

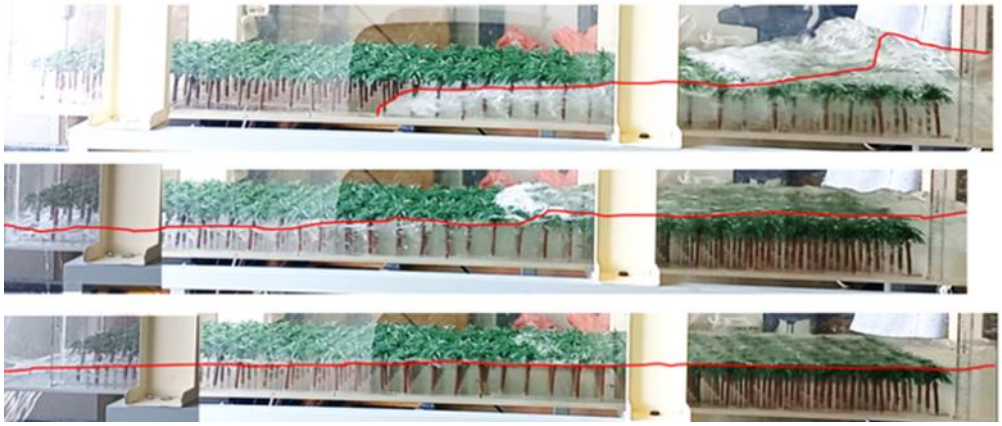

Figure 6. Spatial variation in the depth of flow through a 180 m long forest for a tsunami height of 7 m.

A significant volume of water was blocked by the forest led to the reflection of a large amount of water in the front of the forest. The tsunami did not fully submerge the forest contrary to that of the forest length of 30 m. The flow above the forest was greatly delayed by the roughness of the canopy structure. The turbulent structure was significant in the canopy of trees at

the front of the forest as observed in the forest length of 30 m but gradually decreased and disappeared around the middle of the forest when the velocity of flow decreased. The trees in the front rows were bent by the force of the tsunami, but those in the middle of the forest and behind it did not bend. This means that the trees at the front were subjected to a larger hydrodynamic force than the other trees in the forest. The turbulent structure was significant when the depth of flow was above the height of the canopy, and the velocity of flow was high. A uniform gradient in the level of water was observed through the forest once the flow depth was lower than the canopy height and the tsunami front left the forest.

Fig. 7 (Left panel) shows the maximum flow depth in front of the forest compared to the no forest for tsunami heights. The maximum flow depth increased with tsunami height for no forest conditions. For forest lengths up to 60 m, the forest did not contribute to flow reduction for tsunami heights up to 5 m. Because the flow resistance was generated only from the stems and the porosity between stems was large (Fig. 2c). However, with tsunami heights of 6 and 7 m, the maximum flow depth was doubled in front of the forest compared to the no-forest case. This was due to the flow-canopy interaction. The porosity of the canopy was significantly smaller than that of the stems of the trees. In general, the reflection in front of the forest was negligible for small forest lengths for small tsunamis. The reflection increased with the tsunami height of more than 4 m for the forest length of longer than 90 m. The highest reflection of 14.5 m was measured for the forest length of 180 m for the tsunami height of 7 m. Fig. 7 (Right panel) shows the maximum flow depth behind the forest compared to no forest for tsunami height. Up to the forest length of 120 m, the forest did not show a reduction in the maximum flow depth. However, the forest length longer than 150 m showed a reduction in the maximum flow depth behind the forest. The rate of reduction increased with tsunami height where the maximum flow depth was decreased from 6 m to 3.8 m behind the forest of 180 m length for 7 m tsunami height.

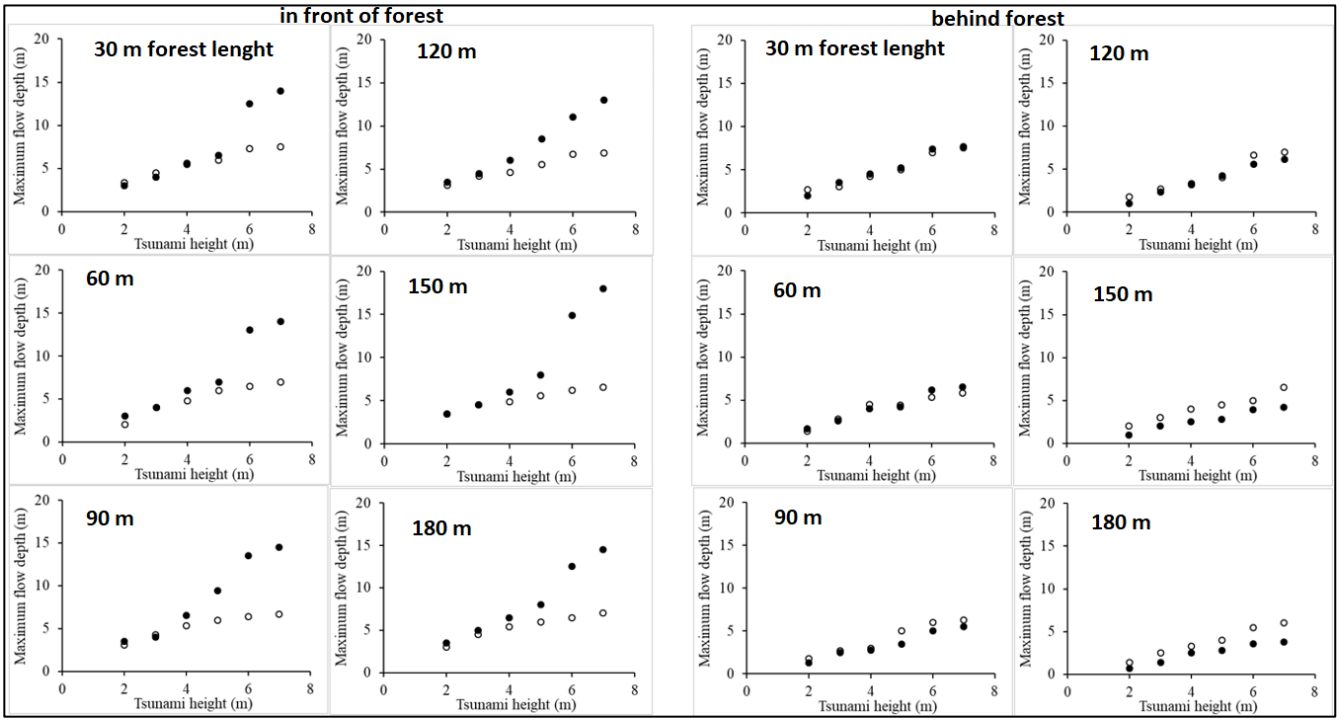

Figure 7. Change in maximum flow depth; Left panel: in front of the forest, Right Panel: behind the forest. Black circles display "with forest" and white circles for "no forest".

3 CONCLUSIONS

Laboratory experiments were conducted to assess the capability of date palm trees to protect from tsunamis. The characteristics of the tsunami and forest were modeled at a geometric scale of 1:100 with Froude-Cauchy similitude. A turbulent, curly flow was apparent when the tsunami flowed through the canopy of the date palm trees but was not observed through the stems of the trees. When a high tsunami passed through a short forest, the turbulent flow was dominant over the entire length of the forest but disappeared before the forest ended when the latter was long. The reflection in front of the forest was negligibly small for tsunami heights less than 4 m, where the maximum depth of flow was below the height of the canopy of the trees. If the maximum depth of flow was above the height of the canopy of the trees the reflection in front of the forest rapidly increased. This confirmed that the canopy played a key role in reducing tsunamis. The maximum reduction in the depth of flow behind the forest was negligibly small for small forest lengths and low tsunamis, however, increased with high tsunamis when the forest was longer than 120 m. When the forest was 180 m long and the tsunami wave was 7 m high, the maximum depth of flow decreased from 6 m to 3.8 m behind the forest.

ACKNOWLEDGEMENT

This study was funded by the SDGs project (G00004062) and UPAR (12N112) of United Arab Emirates University. I would like to thank Dania Hasan, Maryam Alsereidi, Salma Almansoori, and Faisal Karim for their assistance during the experimental study.

REFERENCES

Rovere, E., Casella, D. L., Harris,T., Lorscheid, N.A.K., Nandasena, B., Dyer, M.R., Sandstrom, P., Stocchi, W.J., D'Andrea, M.E., Raymo. 2017. Giant boulders and Last Interglacial storm intensity in the North Atlantic. *Proceedings of the National Academy of Sciences*.

Jordan, B. R. 2008. Tsunamis of the Arabian Peninsula a guide of historic events. *Science of Tsunami Hazards*, 27(1), 31.

Byrne, D. E., Sykes, L. R., Davis, D. M. 1992. Great thrust earthquakes and aseismic slip along the plate boundary of the Makran subduction zone. *Journal of Geophysical Research: Solid Earth*, 97(B1), 449-478.

Pararas-Carayannis, G. 2006 The Potential for Tsunami Generation along the Makran Subduction Zone in the Northern Arabian Sea. Case Study: The Earthquake and Tsunami of November 28, 1945. *Science of Tsunami Hazard*, 24, 358-384.

Estrella, M., Saalismaa, N. 2013. in The Role of Ecosystem Management in Disaster Risk Reduction (eds Renaud, F. et al.), pp. 30–31 (UNU Press, 2013).

Sarker, M.A. 2017. A Review of Numerical Modelling of Cyclones and Tsunamis in the Arabian Sea by Royal HaskoningDHV. *International Journal of Hydrology*, 1:00014.

Suppasri, A., Latcharote, P., Pokavanich, T., Al-salem, K., Al-Enezi, A., Toda, S., Imamura, F. 2016. Tsunami Hazard Assessment for the Arabian Gulf from Earthquakes and Surface Landslides. *Journal of Japan Society of Civil Engineers*, Ser. B2 (Coastal Engineering) 72:1675-1680.

Nouri, M., Namin, M.M., Rashidi, A. 2020. A first-order Landslide Tsunami Hazard Assessment in the Western Makran. *18th Iranian Hydraulic Conference*, 5-6 February 2020.

El-Hussain, I., Omira, R., Al-Bulushi, K., Deif, A., Al-Habsi, Z., Al-Rawas, G., Mohamad, A., Al-Jabri, K., Baptista, M.A. 2017. Tsunami hazard assessment along Diba-Oman and Diba-Al-Emirates coasts. *MATEC Web Conference*, 120:06007.

Rashidi, A., Dutykh, D., Keshavarz, N., Audin, L. 2022. Regional tsunami hazard from splay faults in the Gulf of Oman. *Ocean Engineering*, 243:110169.

Hoffmann, G., Reicherter, K., Wiatr, T., Grutzner, C., Rausch, T. 2013. Block and boulder accumulations along the coastline between Fins and Sur (Sultanate of Oman): tsunamigenic remains? *Nat Hazards*, 65:851–873.

Hoffmann, G., Grützner, C., Reicherter, K., Preusser, F. 2015. Geo-archaeological evidence for a Holocene extreme flooding event within the Arabian Sea (Ras al Hadd, Oman). *Quaternary Science Reviews*, 113:123-133.

Koster, B., Hoffmann, G., Grützner, C., Reicherter, K. 2014. Ground penetrating radar facies of inferred tsunami deposits on the shores of the Arabian Sea (Northern Indian Ocean). *Marine Geology*, 351:13-24.

Griffis, A. 2018. Identifying Overwash Deposits in Arid Environments: Towards a Millennial-Scale Record of Cyclones and Makran Trench Tsunamis from Sur Lagoon, Oman. *Master's Thesis*, The university of southern Mississippi.

Danielsen, F., Sørensen, M.K., Olwig, M.F., Selvam, V., Parish. F., Burgess, N.D., Hiraishi, T., Karunagaran, V.M., Rasmussen, M.S., Hansen, L.B., Quarto, A., Suryadiputra, N. 2005. The Asian tsunami: a protective role for coastal vegetation. *Science*, 310(5748):643.

Kathiresan, K., Rajendran, N. 2005. Coastal mangrove forests mitigated tsunami. *Estuarine Coastal and Shelf Science*, 65:601-606.

Harada, K., Imamura, F. 2005. Effects of Coastal Forest on Tsunami Hazard Mitigation — A Preliminary Investigation. In: Satake, K. (eds) Tsunamis. *Advances in Natural and Technological Hazards Research*, 23.

Tanaka, N., Sasaki, Y. 2007. Limitations of coastal vegetation in the 2004 Indian Ocean tsunami and 2006 Java tsunami. *Proceedings of IAHR 32nd Congress*, (CDROM), Venice, Italy.

Tanaka, N., Sasaki, Y., Mowjood, M.I.M. 2006. Effects of sand dune and vegetation in the coastal area of Sri Lanka at the Indian Ocean tsunami, In: Eds, Namsik Park et al., *Advances in Geosciences 6*, World Scientific Publishing, Co.

Tanaka, N., Sasaki, Y., Mowjood, M.I.M., Jinadasa, K.B.S.N. 2007. Coastal vegetation structures and their functions in tsunami protection: Experience of the recent Indian Ocean tsunami. *Landscape and Ecological Engineering*, 3:33-45.

Nandasena, N.A.K., Tanaka, N., Tanimoto, K. 2008. Tsunami current inundation of ground with coastal vegetation effects; an initial step towards a natural solution for tsunami amelioration. *J. Earthquake and Tsunami*, 2(2):157–171.

Tanaka, N., Jinadasa, K.B.S.N., Mowjood, M.I.M. et al. 2011. Coastal vegetation planting projects for tsunami disaster mitigation: effectiveness evaluation of new establishments. *Landscape Ecol Eng*, 7:127–135.

Iimura, K., Tanaka, N. 2012. Numerical simulation estimating effects of tree density distribution in coastal forest on tsunami mitigation. *Ocean Engineering*, 54:223-232.

Samarakoon, M.B., Tanaka, N., Iimura, K. 2013. Improvement of effectiveness of existing Casuarina equisetifolia forests in mitigating tsunami damage. *Journal of Environmental Management*, 114:105-114.

Tanaka, N., Yasuda, S., Iimura, K., Yagisawa, J. 2014. Combined effects of coastal forest and sea embankment on reducing the washout region of houses in the Great East Japan tsunami. *Journal of Hydro-environment Research*, 8(3):270-280.

Rodríguez, R., Encina, P., Espinosa, M. et al. 2016. Field study on planted forest structures and their role in protecting communities against

tsunamis: experiences along the coast of the Biobío Region, Chile. *Landscape Ecol Eng.* 12:1–12.

Tanaka, N., Onai, A. 2017. Mitigation of destructive fluid force on buildings due to trapping of floating debris by coastal forest during the Great East Japan tsunami. *Landscape Ecol Eng*, 13:131–144.

Torita, H., Igarashi, Y., Tanaka, N. 2022. Effective management of Japanese black pine (Pinus thunbergii Parlat.) coastal forests considering tsunami mitigation. *Journal of Environmental Management*, 311:114754.

Chao, C.T., Krueger, R.R. 2007. The Date Palm (Phoenix dactylifera L.): Overview of Biology, Uses, and Cultivation. *HortScience*, 42:1077-1082.

Munier, P. 1973. Le palmier dattier. Techniques Agricoles et Productions Tropicales. Paris 5eme, Maisonneuve et Larose 217.

Jahromi, M.,K., Jafari, A., Rafiee, S., Jahromi, K.I. 2007. A survey on some physical properties of the Date Palm tree. *Journal of Agricultural Technology*, 317-322.

Amroune, A., Bezazi, A., Belaadi, A., Zhu, C., Scarpa, F., Rahatekar, S., Imad, A. 2015. Tensile mechanical properties and surface chemical sensitivity of technical fibres from date palm fruit branches (Phoenix dactylifera L.). *Composites Part A: Applied Science and Manufacturing*, 71: 95-106.

Chihaoui, B., Serra-Parareda, F., Tarrés, Q., Espinach, F.X., Boufi, S., Delgado-Aguilar, M. 2020. Effect of the Fiber Treatment on the Stiffness of Date Palm Fiber Reinforced PP Composites: Macro and Micromechanical Evaluation of the Young's Modulus. *Polymers*, 12(8):1693.

Jonoobi, M., Shafie, M., Shirmohammadli, Y., Ashori, A., Zarea-Hosseinabadi, H., Mekonnen, T. 2019. A Review on Date Palm Tree: Properties, Characterization and Its Potential Applications. *Journal of Renewable Materials*, 7(11):1055–1075.

Bahtiar, E.T., Nugroho, N., Surjokusumo, S. 2010. Estimating young's modulus and modulus of rupture of coconut logs using reconstruction method. *Civil Engineering Dimension*, 12(2), 65+.

Nurulaini, B., Romli, A.Z., Abidin, M.H. 2013. Tensile and Flexural Properties of Casuarina equisetifolia Unsaturated Polyester Composites. *AMR*, 812:231–5.

Zhang, X., Chua, V.P., Cheong, H. 2015. Hydrodynamics in mangrove prop roots and their physical properties. *Journal of Hydro-environment Research*, 9(2):281-294.

Pestka, A., Kłosowski, P., Lubowiecka, I., Krajewski, M. 2019. Influence of Wood Moisture on Strength and Elastic Modulus for Pine and Fir Wood Subjected to 4-point Bending Tests. *IOP Conference Series: Materials Science and Engineering*, 471(3).

Nandasena, N.A.K., Tanaka, N. 2013. Boulder transport by high energy: Numerical model-fitting experimental observations. *Ocean Engineering*, 57:163-179.

Xu, Z., Melville, B., Whittaker, C., Nandasena, N.A.K., Shamseldin, A. 2021. Mitigation of tsunami bore impact on a vertical wall behind a barrier. *Coastal Engineering*, 164:103833.